Electromagnetic noise suppression characteristics of a coplanar waveguide transmission line integrated with a magnetic thin film

著者	Sohn Jaecheon, Han S. H., Yamaguchi Masahiro, Lim S. H.
journal or publication title	Journal of Applied Physics
volume	100
number	12
page range	124510
year	2006
URL	http://hdl.handle.net/10097/51958

doi: 10.1063/1.2402478

Electromagnetic noise suppression characteristics of a coplanar waveguide transmission line integrated with a magnetic thin film

Jaecheon Sohn and S. H. Han
Nano Device Research Center, Korea Institute of Science and Technology, P.O. Box 131, Cheongryang, Seoul 130-650, Korea

Masahiro Yamaguchi
Department of Electrical and Communication Engineering, Tohoku University, Sendai 980-8579, Japan

S. H. Lim[a)]
Department of Materials Science and Engineering, Korea University, Seoul 136-713, Korea

(Received 14 June 2006; accepted 16 October 2006; published online 28 December 2006)

Integrated-type electromagnetic noise suppressors based on a coplanar waveguide transmission line, incorporated with a SiO_2 dielectric and a nanogranular Co–Fe–Al–O magnetic thin film with excellent high frequency soft magnetic properties, are reported. A systematic study on the frequency dependences of scattering parameters, power loss, and phases of transmitted and reflected signals as a function of the length and width of the magnetic thin film indicates that the main loss mechanism of the integrated devices is the *L-C* resonance. Excellent noise suppression characteristics, combined with a resonance frequency of several gigahertz, are achieved in the present integrated devices. © *2006 American Institute of Physics*. [DOI: 10.1063/1.2402478]

I. INTRODUCTION

Electromagnetic noise in integrated circuits continues to be problematic as the operational frequency and degree of integration of electronic devices increase continuously. A good example is wireless communications devices of extremely compact design with their operational frequency nowadays reaching the gigahertz range. The frequencies of electromagnetic noise can be even higher with the generation of harmonics. The fundamental operational frequency combines with harmonics to form repetitive nonsinusoidal distorted waves, causing the different frequencies to flow back on the electrical system, even though they do not perform any useful work. These harmonics reduce current capacity on the wiring system, causing overheating of electrical apparatus, and, in some cases, they even disturb normal voltages causing serious electromagnetic wave interference, eventually leading to dysfunction of electronic devices. Even more complicated frequencies can be formed through the combination of harmonics themselves, called intermodulation distortion. Considering an overwhelming tendency of increasing frequency and device integration, it is important to address problems related to electromagnetic noise.

Magnetic materials have played an important role in tackling this problem. Electromagnetic noise suppressors based on Co–Zr–Nb and Co–Pd–Al–O sputtered magnetic films[1–3] and spin sprayed Ni–Zn–(Co) soft ferrite films[4] were previously reported. The device structure mainly consisted of a coplanar waveguide (CPW) transmission line covered with a magnetic thin film. In this type of noise suppressors, unwanted noises (usually harmonics in power circuits) are mainly absorbed by the loss generation due to ferromagnetic resonance (FMR). Recently, the present authors reported a similar, nonintegrated-type noise suppressor[5] incorporated with a nanogranular Co–Fe–Al–O thin film.[6–8] The device was considered to be promising, confirming the suitability of the Co–Fe–Al–O thin film as a high frequency noise suppressor. However, a small magnitude of noise absorption was observed from the device due to a large separation between the CPW transmission line and the magnetic thin film, which can be expected from the nonintegrated nature of the device.

Very recently, integrated-type noise suppressors were fabricated in an effort to solve the problem of small noise absorption.[9] Expectedly, large signal attenuation was achieved in the integrated devices, and, furthermore, the resonance frequency is in the range of 10 GHz, being much higher than the FMR frequency of 2.24 GHz observed in the Co–Fe–Al–O thin film. Later, it was found that the main mechanism of the loss generation is the *L-C* resonance, and not FMR observed previously in similar devices. This change in the mechanism of the loss generation occurs due to increased distributed capacitance and inductance resulting from much reduced separation between the magnetic thin film and the transmission line (0.1–0.5 μm). In this work, more detailed results are reported, with particular emphasis given on the effects of the length (l) and width (w) of the magnetic thin film.

II. EXPERIMENTS

Following the Muller-Hillberg equations,[10] a CPW transmission line with a characteristic impedance of 50 Ω was designed for a signal linewidth of 50 μm and a thickness of 3 μm on a 7059 Corning glass substrate.[1–3,5] A cross-sectional view of the designed transmission line is shown in Fig. 1(a) together with the dielectric (SiO_2) and magnetic layers. A schematic showing the overall device structure is

[a)]Author to whom correspondence should be addressed; FAX: 82-2-928-3584; electronic mail: sangholim@korea.ac.kr

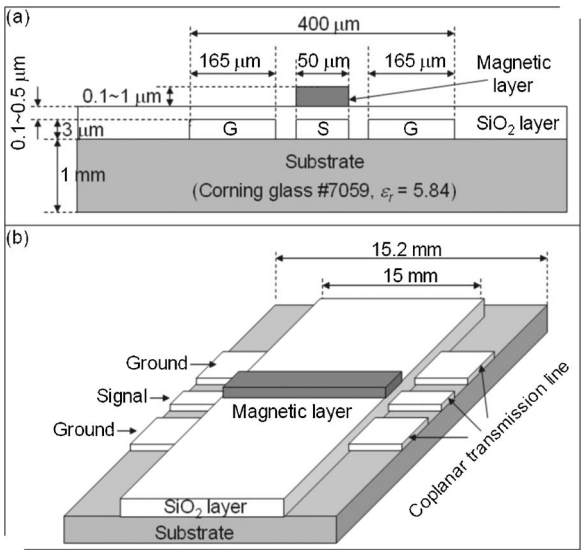

FIG. 1. (a) A cross-sectional view of the CPW transmission line and the dielectric and magnetic layers (with detailed dimensions). (b) A schematic showing the overall device structure. The illustrations are for a magnetic thin film with a width of 50 μm (the same as the signal linewidth) and a length of 15 mm. Note that the dimensions are not in a proper scale.

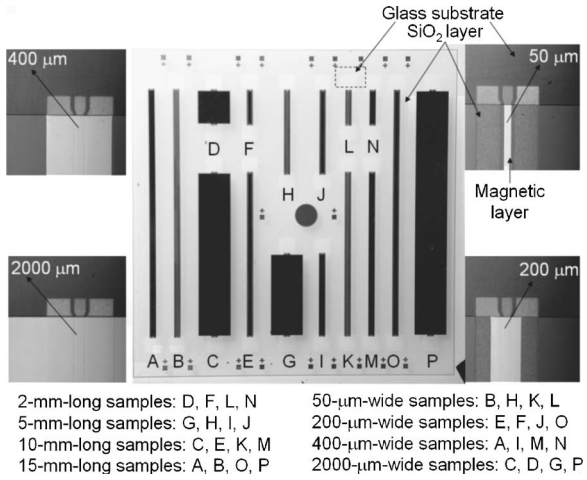

FIG. 2. A total of 16 samples with various *lateral* dimensions, which are obtained from each run of fabrication. Also shown is a magnified portion near the contact for four different widths of the magnetic thin film.

displayed in Fig. 1(b). Note that the dimensions in Figs. 1(a) and 1(b) are not in a proper scale. The overall stack consisted of the Co–Fe–Al–O magnetic thin film (1 μm)/SiO_2 (0.1 μm)/Cu transmission line (3 μm)/glass substrate (1 mm). A conventional microfabrication process including photolithography was used to fabricate the integrated noise suppressor. The Cu transmission lines were deposited by electroplating in an electrolyte composed of $CuSO_4$, H_2SO_4, and de-ionized (DI) water. Before the Cu plating, very thin seed layers of Cu (0.06 μm)/Ti (0.01 μm) were deposited by rf sputtering onto the glass substrate. Also, a very thin Ti layer with a thickness of ~10 nm was deposited between the SiO_2 layer and magnetic thin film for an improved adhesion of the magnetic layer onto the SiO_2 layer. A nanogranular magnetic film with the composition $Co_{41}Fe_{38}Al_{13}O_8$ (in at. %) was deposited by rf magnetron sputtering under a static magnetic field of 1 kOe to form an induced anisotropy.[5,7,8] After photoresist patterning, the magnetic film was etched by ion milling. Finally, a wet etching method was used to remove the SiO_2 layer on the contact pad at both ends of the transmission line by using a buffered oxide etch solution ($HF:H_2O=1:6$). A total of 16 samples with various *lateral* dimensions were obtained from each run of fabrication, as can be seen from Fig. 2. The difference in the length of the magnetic thin film (and also the transmission line) is obvious from Fig. 2, and there are four different lengths of the magnetic thin films: 2, 5, 10, and 15 mm. Note that the length of the Cu transmission line is longer than that of the dielectric and magnetic thin films by 0.2 mm to provide room for electrical contacts. For each length, there are four different widths of the magnetic thin film: 50 μm (the same as the Cu signal linewidth), 200 μm, 400 μm, and 2000 μm. A magnified portion of the device near the contact (the end of the transmission line) is also shown in Fig. 2 for four different widths of the magnetic thin film. It is clear from the magnified photos that, at the width of 50 μm, the magnetic thin film only covers the signal line and, at the width of 400 μm or greater, it completely covers both the signal and ground lines. For measurements, two ground-signal-ground (GSG) pin-type wafer probes were in mechanical contact with both ends of the CPW transmission line. The *S* parameters (S_{11} and S_{21}) were measured with an HP 8720D network analyzer in the frequency range of 0.1–20 GHz.

III. RESULTS AND DISCUSSION

The present $Co_{41}Fe_{38}Al_{13}O_8$ nanogranular thin film exhibits excellent soft magnetic properties at high frequencies and important properties are summarized as follows:[5,7,8] an electrical resistivity (ρ) of 374 $\mu\Omega$ cm, an anisotropy field (H_K) of 50 Oe, a hard axis coercivity of 1.25 Oe, a saturation magnetization ($4\pi M_S$) of 12.9 kG, and a resonance frequency (f_R) of 2.24 GHz.

Figures 3(a) and 3(b), respectively, show the frequency dependences of the transmitted (S_{21}) and reflected (S_{11}) scattering parameters and the fraction of power loss (P_{loss}/P_{input}) for the bare CPW transmission lines with various lengths of 2, 5, 10, and 15 mm. Here, P_{loss} and P_{input} denote the power loss and input power, respectively. Figures 3(c) and 3(d), respectively, show the results for the phase angle (in degrees) of the transmitted and reflected signals. It is worth noting here that the real length of the transmission line is longer than the specified length by 0.2 mm, as was mentioned in the previous section, but the length is indicated by the specified length in this paper simply for convenience: for example, 2 mm not 2.2 mm. In all cases, the attenuation of the transmitted signal is relatively small over the whole frequency range (at low frequencies in particular) investigated in this work. The difference in S_{21} depending on the line length is not clearly visible except for the frequency range higher than 10 GHz where, for a given frequency, the signal attenuation increases progressively with increasing line length. Obviously, in the bare structure, the signal attenuation is mainly due to Ohmic loss caused by the conductive elements of the bare CPW line itself and accordingly the results for S_{21} [Fig. 3(a)] can be well understood.

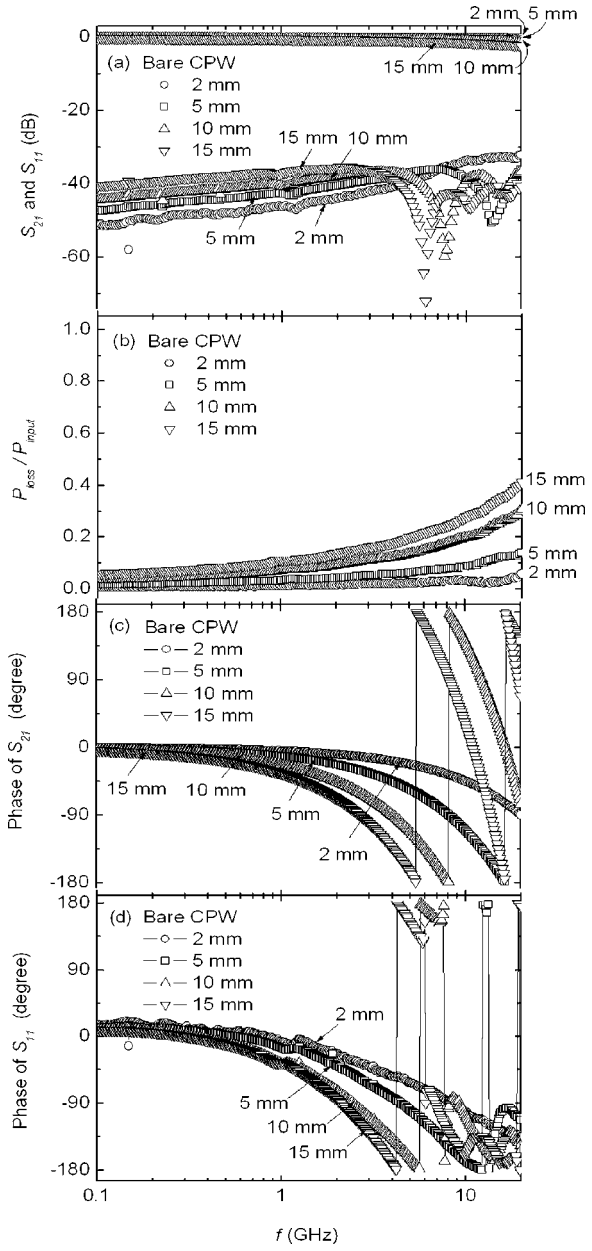

FIG. 3. The frequency dependences of (a) the transmitted (S_{21}) and reflected (S_{11}) scattering parameters, (b) the fraction of power loss ($P_{\text{loss}}/P_{\text{input}}$), (c) the phase angle (in degrees) of the transmitted signals, and (d) the phase angle (in degrees) of the reflected signals for the bare CPW transmission lines with various lengths of 2, 5, 10, and 15 mm.

The amount of reflected signal (S_{11}) is also very small being less than −30 dB in all cases. At low frequencies, the magnitude of reflected signal is higher at longer CPW transmission line length and, at a given length, it increases slowly with increasing frequency. At high frequencies, however, no obvious tendency is seen, mainly due to the appearance of sharp minima (dips) in S_{11}. The number of these dips increases progressively with increasing line length; it is none at $l=2$ mm, one at $l=5$ mm, two at $l=10$ mm, and three at $l=15$ mm. These dips are known to be caused by dimensional resonance which occurs when $l=(n)(\lambda_g/2)$, where n is the natural number (1, 2, 3,…) and λ_g is the guided wavelength.[11–14] In the case of $l=15$ mm (more precisely 15.2 mm) with three dips, the first strongest dip, observed at a frequency of 5.84 GHz, occurs at $n=1$ and the next two dips at higher frequencies occur at higher n values of 2 and 3. At the strongest dip, the guided wavelength (λ_g) is calculated to be 30 mm and this value can be compared with the wavelength of the electromagnetic wave in the free space at the same frequency of 5.84 GHz ($\lambda=51$ mm). It is clear that the wavelength of the electromagnetic wave along the Cu transmission line is shortened (from 51 to 30 mm) and this is mainly due to the interaction of the electromagnetic wave with the dielectric glass substrate. The calculated value of the guided wavelength from the dip (30 mm), however, is substantially greater than the value predicted from the equation $\lambda_g=\lambda/\varepsilon_r^{1/2}$ (21.1 mm), where ε_r is the relative dielectric constant of the glass substrate ($\varepsilon_r=5.84$). This deviation can be understood because the equation for the guided wavelength ($\lambda_g=\lambda/\varepsilon_r^{1/2}$) applies to the case when the electromagnetic wave travels *through* the medium (glass). In the present case, the electromagnetic wave travels through the Cu transmission line being located on the glass substrate. So, the interaction of the electromagnetic wave with the glass substrate will not occur in full, resulting in less shortening of the electromagnetic wave. It is seen from Figs. 3(a) and 3(d) that, during the dimensional resonance, an abrupt change in the phase of the reflected signal occurs and this is most obvious for the strongest dip in S_{11} (at $n=1$) where a large discontinuous change (drop) of the phase occurs in the reflected signal. The phase shift tends to increase with decreasing l. At higher orders, the phase change is small and also continuous. In the case of transmitted signal, no abrupt phase change occurs, as can be seen from Fig. 3(c).

The fraction of power loss can be calculated from the scattering parameters by using the equation $P_{\text{loss}}/P_{\text{input}}=1-(|S_{21}|^2+|S_{11}|^2)$. As can be expected from the results for S_{21} and S_{11}, the power loss is higher at longer line length. At a given length, the power loss increases progressively with increasing frequency in a *parabolic* manner, this behavior being most prominent at the longest length of 15 mm. The power loss observed at the highest measured frequency of 20 GHz is actually not small; the fraction of power loss is about 40% at $l=15$ mm, even for the bare CPW transmission line.

Figures 4(a)–4(c), respectively, show the frequency dependences of S_{21}, S_{11}, and $P_{\text{loss}}/P_{\text{input}}$ for the integrated noise suppressors with varying lengths of the magnetic thin film; $l=2$, 5, 10, and 15 mm. The thickness of the SiO_2 dielectric layer was fixed at 0.1 μm. The thickness and width of the magnetic thin film were maintained constant at 1 and 50 μm, respectively. Essentially, the integrated devices were formed onto the bare transmission lines, discussed just before, by depositing a 0.1 μm thin SiO_2 dielectric layer, followed by a 1 μm thin magnetic thin film covering only the signal line. A comparison of the results for the scattering parameters between the bare transmission lines [Fig. 3(a)] and the present devices integrated with the dielectric and magnetic thin films [Figs. 4(a) and 4(b)] clearly indicates a significant difference. At low frequencies below 1 GHz, no substantial difference is visible in the signal attenuation depending on the length of the magnetic thin film. However, a significant difference is clearly visible at high frequencies, mainly due to large dips

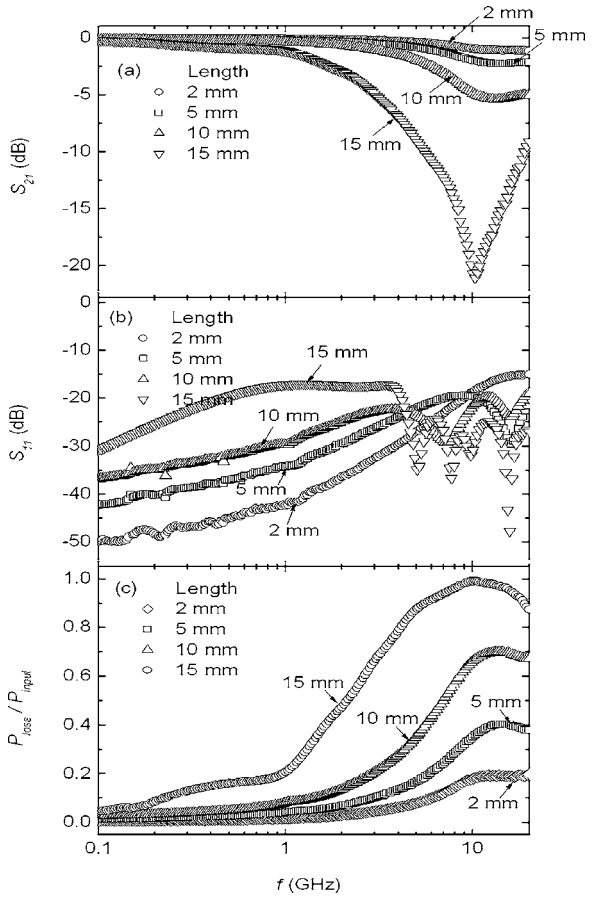

FIG. 4. The frequency dependences of (a) the transmitted (S_{21}) and (b) reflected (S_{11}) scattering parameters and (c) the fraction of power loss ($P_{\text{loss}}/P_{\text{input}}$) for the integrated noise suppressors with varying lengths of the magnetic thin film of 2, 5, 10, and 15 mm. The thickness of the SiO_2 dielectric layer was fixed at 0.1 μm. The thickness and width of the magnetic thin film were maintained constant at 1 and 50 μm, respectively.

in S_{21} occurring at frequencies higher than 10 GHz. This dip in S_{21}, indicating a large signal absorption at a specific frequency, is typical of resonance and this resonance behavior is more prominent at longer lengths. The magnitude of signal attenuation increases with increasing length of the magnetic thin film (also the Cu signal and ground lines). The increase is particularly prominent as the length increases from 10 to 15 mm; at the minimum dips, the value of S_{21} is -5 to -6 dB at $l=10$ mm, but it is decreased to -21 dB at $l=15$ mm. The resonance frequency is roughly in the range of 10 GHz, except for $l=2$ mm where no obvious resonance occurs in the measured frequency range. A close examination shows that the resonance frequency tends to decrease with increasing length; it is 12.6 GHz at $l=5$ mm, 12 GHz at $l=10$ mm, and 10.2 GHz at $l=15$ mm. The present results for the change in the signal attenuation and the resonance frequency as a function of the length can be understood because distributed components of both L and C are expected to increase with increasing length.[9]

An overall behavior of reflected signal (S_{11}) is similar to that for the bare transmission lines. This is particularly true for the occurrence of sharp minima (dips) in S_{11}. No change in the number of dips is observed except for $l=15$ mm where the number of dips is increased to 4 from 3 for the bare structure. The position of the dips is slightly different, although this is not very clear from the figures. A closer examination shows that the frequency at which the dip occurs is shifted towards the lower frequency side. For example, at the lowest order of $n=1$, the frequency is decreased to 4.96 from 5.84 GHz at $l=15$ mm. This indicates that the guided wavelength is shortened even further with the incorporation of the dielectric and magnetic layers, which can be understood because the electromagnetic wave further interacts with these additional layers as well as the dielectric glass substrate. A conspicuous difference, as compared with the bare transmission lines, is the increased signal reflection and this is clearly seen at $l=15$ mm. In this length, the signal reflection is substantially high even in the low frequency range. The highest signal reflection occurs at about 1 GHz where the magnitude of S_{11} is about -17 dB. This can be compared with the value of -36 dB for the bare transmission line at the same frequency.

With the increased signal attenuation and reflection as the dielectric and magnetic thin films are incorporated, it is readily expected that the power loss also increases. This expectation is well met by the results for the power loss shown in Fig. 4(c). For a given frequency, the power loss increases progressively with increasing length. In the case of a given length, the frequency dependence initially shows a parabolic behavior similarly to the bare transmission lines, followed by maxima ($l=5,10,15$ mm) or plateau ($l=2$ mm) at frequencies close to 10 GHz. At the maximum point, the fraction of the power loss with respect to the input power reaches nearly 100% at $l=15$ mm and over 70% at $l=12$ mm. Obviously, the maximum points are related to the resonance, and this is confirmed by the fact that these maximum points indeed completely coincide with the dips in S_{21}. At the largest length of $l=15$ mm, the power loss begins to increase at 1 GHz, and this behavior is in good accord with the frequency dependence of the signal attenuation shown in Fig. 4(a) from which it is seen that, at the same frequency of 1 GHz, the signal attenuation begins to increase. This fact further demonstrates the good correlation between the scattering parameters and power loss.

The results shown in Figs. 4(a)–4(c) indicate good signal attenuation characteristics at the longest length of $l=15$ mm. In order to further improve the noise absorption characteristics, the width of the magnetic thin film (w) was increased from 50 up to 2000 μm, while the length was fixed at $l=15$ mm. The rest of the parameters were the same as before. The results for the frequency dependence of the scattering parameters and power loss are shown in Figs. 5(a)–5(c) for $w=50$, 200, 400, and 2000 μm in a way similar to Figs. 4(a)–4(c). It is reminded that, at $w=50$ μm, the magnetic thin film only covers the signal line; on the other hand, at $w=200$ μm, the magnetic film also covers a part (about 40%) of the ground lines as well as the signal line and it completely covers both the signal and ground lines at $w \geqslant 400$ μm [see Fig. 1(a)]. The amount of signal attenuation is greatly increased as the width increases from 50 to 200 μm while the resonance frequency is decreased. It is interesting to see that there are two minima at $w=200$ μm in the frequency dependence of S_{21}, although the

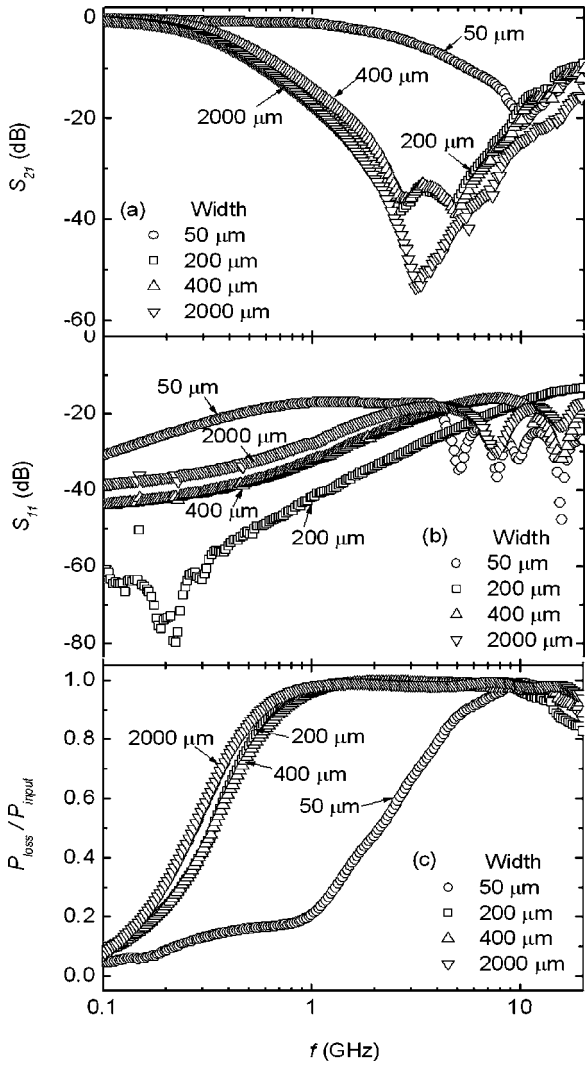

FIG. 5. The frequency dependences of (a) the transmitted (S_{21}) and (b) reflected (S_{11}) scattering parameters and (c) the fraction of power loss ($P_{\text{loss}}/P_{\text{input}}$) for the integrated noise suppressors with varying widths of the magnetic thin film of 50, 200, 400, and 2000 μm. The thickness of the SiO_2 dielectric layer was fixed at 0.1 μm. The thickness and length of the magnetic thin film were maintained constant at 1 μm and 15 mm, respectively.

reason is not clearly understood at the moment. However, these two minima have similar values and the maximum connecting the two minima (the peak to valley height) is small, so the overall shape appears like a plateau. The value of S_{21} in this plateau, which spans in the range of 2.6–4.7 GHz, is −33 to −38 dB. This value is much smaller than the value of −18 dB observed at $w=50$ μm. In addition to the resonance frequency, the frequency at which an appreciable signal attenuation occurs is decreased greatly at $w=200$ μm; it is 100–200 MHz, a large reduction from the value of 1 GHz at $w=50$ μm. No appreciable change occurs as the width increases from 200 to 400 μm; in fact, the frequency dependence of S_{21} is very similar to each other over the whole frequency range. The similarity includes the existence of the plateau being composed of two minima. As the width increases from 400 to 2000 μm, the amount of the signal attenuation is further increased; over the whole frequency range, the value of S_{21} is the lowest, the difference being greatest near the resonance frequency. No two minima but a typical single dip in S_{21} is observed at this largest width and the resonance frequency appears to be reduced, although this is not clear, mainly due to the double dips at the smaller widths of $w=200$ and 400 μm.

Let us now consider the change in the signal attenuation characteristics as a function of the width of the magnetic thin film. Since the *L*-*C* resonance is expected to play a main role in the loss generation, the present results can also be explained by the change in *L* and *C* as a function of the width. The major contribution to *C* comes from the capacitor composed of the signal line/SiO_2 dielectric layer/magnetic thin film. Minor contributions are expected from the interactions between the signal and ground lines and between the ground lines and magnetic thin film. When the width of the magnetic thin film is equal or smaller than the signal linewidth (namely, $w \leqslant 50$ μm), the value of *C* is expected to increase linearly with the width of the magnetic thin film, since the distributed capacitance is proportional to the area of the capacitor. However, this linear increase is not expected at $w \geqslant 50$ μm, since the effective contribution by a given increase of the width is expected to decrease as the width of the magnetic thin film exceeds the signal linewidth of 50 μm. Eventually, the increase of the capacitance becomes saturated at a certain value of *w* and it can be estimated from the present results that the saturation occurs in the range $50\ \mu\text{m} \leqslant w \leqslant 200\ \mu\text{m}$. The value of *L* is related to the magnetic volume, namely, the width of the magnetic thin film for a fixed length. In this case also, the distributed inductance will increase linearly with increasing width of the magnetic thin film at $w \leqslant 50$ μm, while, at $w \geqslant 50$ μm, the inductance increase at a given width slows down and finally saturates. This situation corresponds to the physical picture that the magnetic thin film within a certain region near the center only responds to the magnetic field arising from the signal line and the outside region behaves like a nonmagnetic material contributing zero distributed inductance. Actually, this behavior was observed previously in a nonintegrated-type noise suppressor,[5] where the "effective" width of the magnetic thin film over which the magnetic response occurs is greater than the signal linewidth by about 20%. In the present integrated devices, the effective width is expected to be higher. This is because the separation between the signal line and the magnetic thin film is much closer and much higher magnetic field is expected to reach the magnetic thin film from the signal line.

The width dependence of the signal reflection characteristics is not straightforward but rather complex. At low frequencies, the magnitude of reflected signal is highest at the smallest width ($w=50$ μm) and then becomes lowest as the width is increased to 200 μm. Then, the signal reflection increases with increasing width, but the magnitude at the largest width of 2000 μm is smaller than that at the smallest width of 50 μm. This width dependence of S_{11} is different from that observed in other integrated devices, as shown in Figs. 3(a) and 3(b), for example, where the magnitude of reflected signal is high at a condition where the signal attenuation is high. Similar results were also reported in the literature.[1–4] Although the reason for the present width dependence of S_{11} is not known, this is good for applications

since, at a certain width, large signal attenuation combined with small reflection can be achieved. The present results indicate that the best candidate for applications is the noise suppressor with $w=200$ μm, where signal attenuation is relatively large but signal reflection is very small. Again, at high frequencies, no obvious tendency is seen, mainly due to the appearance of sharp minima (dips) in S_{11}. In all case, the level of S_{11} is below -10 dB over the whole frequency range and this value is considered to be good enough for practical applications. The value of -10 dB indicates that the fraction of reflected signal to the total input is 31.6% ($10^{-10/20}$). In general, the acceptable values of S_{11} are below -10 dB for electromagnetic noise suppression applications.[15]

Some change occurs in the frequency dependence of the power loss as the width increases. Unlike the result at $w=50$ μm where the power loss is maximum at the resonance frequency, the power loss at larger widths ($w=200$, 400, and 2000 μm) gradually increases with increasing frequency until 700–800 MHz above which saturation occurs, resulting in a plateau. At this saturation, the $P_{\text{loss}}/P_{\text{input}}$ ratio approaches 100%. This plateau in the power loss at the large widths, not a maximum usually observed in other similar devices as well as at $w=50$ μm, appears not easy to understand, considering that $P_{\text{loss}}/P_{\text{input}}=1-(|S_{21}|^2+|S_{11}|^2)$. However, this can be understood because the power loss results are plotted in a linear scale, while the scattering parameters, expressed in decibels, essentially represent the logarithm scale.

Finally, we wish to mention about the magnetic effect of the electromagnetic noise suppression. Although the magnetic thin film is a part of the capacitor composed of the signal line/SiO_2 dielectric layer/magnetic thin film, its main role is to provide the inductance. Since the value of L is proportional to the permeability, it is important to have a magnetic thin film with a high permeability at the frequency of current interest. In this case, the present devices can have an additional important advantage in that their attenuation characteristics including the resonance frequency can be tuned during the device operation by applying a magnetic field, since the magnitude of distributed inductance can be modulated with the applied magnetic field. This effect will be stronger at larger thickness of magnetic thin film.

IV. CONCLUSIONS

A conventional microfabcication process has been used to fabricate integrated-type electromagnetic noise suppressors incorporated with a SiO_2 dielectric and a nanogranular Co–Fe–Al–O magnetic thin film with excellent high frequency soft magnetic properties. The frequency dependences of the scattering parameters, power loss, and phases of transmitted and reflected signals are systematically investigated over a wide frequency range of 0.1–20 GHz as a function of the length and width of the magnetic thin film. The present study further demonstrates that the main loss mechanism is the L-C resonance. Excellent noise absorption characteristics are achieved, particularly when the length of the magnetic thin film is large (15 mm) and the width of the magnetic thin film exceeds the transmission signal linewidth. At these conditions, the power loss approaches 100% at frequencies well below 1 GHz and the resonance frequency is in the range of several gigahertz, slightly reduced from 10 GHz observed at shorter length and smaller width. It is considered that the present integrated devices are promising as an electromagnetic noise suppressor for information technology (IT) devices such as mobile phones with the operational frequency approaching the gigahertz range.

ACKNOWLEDGMENTS

This work was supported by the Korean Ministry of Science and Technology through the National Research Laboratory program and the Korea-Italy international cooperation research program.

[1] M. Yamaguchi, K.-H. Kim, T. Kuribara, and K.-I. Arai, IEEE Trans. Magn. **37**, 3183 (2002).
[2] K. H. Kim, M. Yamaguchi, K. I. Arai, H. Nagura, and S. Ohnuma, J. Appl. Phys. **93**, 8002 (2003).
[3] K. H. Kim, M. Yamaguchi, S. Ikeda, and K. I. Arai, IEEE Trans. Magn. **39**, 3031 (2003).
[4] K. H. Kim, M. Yamaguchi, K. I. Arai, N. Matsushita, and M. Abe, Trans. Magn. Soc. Jpn. **3**, 133 (2003).
[5] J. C. Sohn, S. H. Han, K. H. Kim, M. Yamaguchi, and S. H. Lim, J. Magn. Magn. Mater. (to be published).
[6] S. Ohnuma, N. Kobayashi, T. Masumoto, S. Mitani, and H. Fujimori, J. Appl. Phys. **85**, 4574 (1997).
[7] J. C. Sohn, D. J. Byun, and S. H. Lim, J. Magn. Magn. Mater. **272–276**, 1500 (2004).
[8] J. C. Sohn, D. J. Byun, and S. H. Lim, Phys. Status Solidi A **201**, 1786 (2004).
[9] J. C. Sohn, S. H. Han, M. Yamaguchi, and S. H. Lim, Appl. Phys. Lett. **89**, 103501 (2006).
[10] B. C. Wadell, *Transmission Line Design Handbook* (Artech House, Boston, 1991), Chap. 3.
[11] W. Barry, IEEE Trans. Microwave Theory Tech. **34**, 80 (1986).
[12] W. B. Weir, Proc. IEEE **62**, 33 (1974).
[13] A. M. Nicolson and G. F. Ross, IEEE Trans. Instrum. Meas. **19**, 377 (1970).
[14] R. W. Ziolkowski, IEEE Trans. Antennas Propag. **51**, 1516 (2003).
[15] K. C. Gupta, R. Greg, I. Bahl, and P. Bhartia, *Microstrip Lines and Slotlines*, 2nd ed. (Artech House, London, 1996), Chap 2.